coatings

MDPI

Article

Slip Factors of Coated Faying Surfaces in High-Strength Bolted Connections: Experimental Evaluation and Code Implications

Linfeng Lu *, Zeyang Yu, Mengyang Liu, Jie Pei and Songlin Ding

School of Civil Engineering, Chang'an University, 75 Chang'an Middle Rd., Xi'an 710064, China; 2025128065@chd.edu.cn (Z.Y.); 2025128057@chd.edu.cn (M.L.); 2025228020@chd.edu.cn (J.P.); 2021128017@chd.edu.cn (S.D.)

* Correspondence: lulinfeng@chd.edu.cn

Abstract

To evaluate the slip resistance of high-strength bolted friction-type connections subjected to different corrosion-protection treatments, calibration tests were performed on six representative faying-surface conditions: sand-blasted (uncoated), epoxy zinc-rich primer, waterborne inorganic zinc-rich coating, alcohol-soluble inorganic anti-corrosion anti-slip primer, a complete multi-layer protective coating system, and cold galvanizing. Fifteen test groups comprising 45 tensile specimens were examined to determine slip factors, which were then compared with values recommended in domestic and international design standards. The results show that sand-blasted surfaces (W type) exhibit stable slip factors of $\mu = 0.43–0.45$; alcohol-soluble inorganic primer surfaces (S type) provide the highest slip resistance with $\mu = 0.49–0.51$, representing an increase of approximately 13%–18% compared with sand-blasted surfaces; and cold-galvanized surfaces (D type) achieve favourable performance with $\mu \approx 0.44$. Waterborne inorganic zinc-rich surfaces (A type) yield $\mu \approx 0.33$, corresponding to a reduction of about 25%, and are suitable for non-slip-critical connections. In contrast, epoxy zinc-rich primers (C type) and complete multi-layer coating systems (X type) present lower slip factors of $\mu = 0.26–0.28$ and $\mu \approx 0.23$, corresponding to reductions of approximately 35%–45% and about 50%, respectively, indicating that the X-type treatment is unsuitable for slip-critical applications. The influence of bolt diameter is limited, with slip-factor variations within 5%–8% under the same surface condition, and no statistically significant effect confirmed by two-way ANOVA. These findings provide a quantitative experimental basis for the design, classification, and future standardization of friction-type bolted connections with coated faying surfaces.

Keywords: high-strength bolted connections; faying surface treatment; slip factor; anti-corrosion coatings; friction behaviour; code applicability

Check for updates

Academic Editors: Giorgos Skordaris and Paolo Castaldo

Received: 25 November 2025
Revised: 20 December 2025
Accepted: 29 December 2025
Published: 2 January 2026

Copyright: © 2026 by the authors. Licensee MDPI, Basel, Switzerland. This article is an open access article distributed under the terms and conditions of the Creative Commons Attribution (CC BY) license.

1. Introduction

High-strength bolted slip-critical (friction-type) connections are widely used in steel structures, particularly in bridges, high-rise buildings, and industrial facilities, where loads are transferred through friction to ensure overall structural stability. The slip factor is a key parameter for assessing the performance of such connections, as it characterizes the slip resistance between the faying surfaces and directly governs the joint's load-carrying capacity and safety. To guarantee long-term service reliability, the faying surfaces must maintain adequate slip resistance. However, sand-blasted surfaces, commonly used in practice, are often affected by environmental factors such as temperature fluctuations,

humidity, and corrosion. These effects can degrade surface quality and reduce interfacial friction, thereby lowering the slip factor and increasing the risk of connection failure [1–4].

To counteract corrosion, protective coatings and paints are frequently applied to the faying surfaces of bolted joints, aiming to enhance surface durability and stability while preserving shear resistance [5]. Previous studies have shown that although anti-corrosion coatings can effectively mitigate corrosion-induced degradation, they can also affect the slip factor in two ways. Our earlier work indicated that external protective paints alone cannot prevent a 4.9%–19% loss of shear capacity in high-strength bolted connections under corrosion, whereas appropriately protected coated faying surfaces can substantially delay such deterioration. Therefore, a systematic investigation of the effects of different coatings or paints on slip factors is essential for structural safety [3].

The latest Chinese standard (T/CSCS 056-2024) [5] explicitly requires that the slip factor of coated faying surfaces should not be lower than the value required by structural design. Many design codes also provide recommended slip factors for commonly used surface treatments [6–10]. Nevertheless, with the rapid application of novel anti-corrosion coatings and treatment technologies, the slip-factor data covered in current standards remains insufficient and cannot meet the increasingly diverse engineering requirements. Accurate determination and calibration of slip factors for coated surfaces are thus crucial for structural design, performance assessment, and durability prediction.

Various researchers have carried out relevant studies. Annan and Chiza [11] investigated the slip behaviour of connections with combined one-sided metallized and one-sided hot-dip galvanized surfaces and found that roughened or wire-brushed galvanized surfaces can achieve slip factors exceeding those specified in standards. Wang et al. [12–14] examined the influence of inorganic zinc-rich coatings, reporting slip factors lower than those of sand-blasted surfaces, and noting that an 80 μm coating produced slightly higher values than a 60 μm coating. In contrast, Mahmoudi et al. [15] showed that for conventional protective paint systems, increasing coating thickness from 20 to 40 μm resulted in a pronounced reduction in the slip factor, with a maximum decrease of 36%. Both studies highlighted the sensitivity of slip performance to coating thickness, yet their conclusions differ, indicating the need for further clarification. Cao Xin [16] tested sand-blasted–arc-sprayed aluminum surfaces and zinc-rich anti-slip coated surfaces on Q500qE steel, obtaining slip factors of 0.70 and 0.60, respectively—significantly higher than current code recommendations [8–10]. Collini et al. [17] reported that non-standard steels, such as COR-TEN and galvanized plates, correspond to Class C surfaces in BS EN 1090-2:2018 [9] and generally exhibit relatively low slip resistance. In addition, research has expanded to high-strength steels, stainless steels, and aluminum–stainless steel hybrid interfaces, further exceeding the scope of existing standards [18–20]. Zhang et al. [20] studied aluminum alloy–stainless steel faying surfaces with different mechanical and metallic coatings and showed that surface roughness, coating thickness, and hardness jointly govern the frictional response, indicating that the slip-factor classifications in EN 1090-2 and JGJ 82 do not apply to non-carbon-steel substrates. Han et al. [21] further demonstrated that, under fretting fatigue, both faying-surface treatment and bolt pretension significantly affect the evolution of the mean slip coefficient. Takai [22] developed a contact-pressure-dependent friction model for joints with inorganic zinc-rich coatings and revealed that the slip coefficient decreases with increasing contact pressure, while splice plate thickness affects slip behaviour through pressure redistribution. From a construction practice perspective, Georgiev [23] showed that using the theoretical torque factor K1 instead of the calibrated K2 leads to large scatter in slip-factor results, and that mistreatment of the paint followed by mechanical cleaning reduces the slip factor by about 12%–18%. Fuente et al. [24] demonstrated that differences in test specimen geometry

among international standards can cause more than 40% variation in effective friction area, explaining why slip factors obtained under different codes are not directly transferable.

In summary, although previous studies have provided valuable preliminary data on the slip performance of coated faying surfaces, standardized testing for new coating products and diverse coating systems remains limited. Current codes and standards [6–10] provide only restricted slip-factor provisions and are insufficient for design under variable environmental and material conditions. To narrow the gap between code provisions and engineering practice, systematic calibration tests of slip factors are urgently required [25].

Accordingly, this study investigates standard high-strength bolted friction-type connections with six representative faying-surface treatments: (1) sand-blasting (or shot blasting); (2) epoxy zinc-rich primer; (3) alcohol-soluble inorganic bridge-specific anti-corrosion anti-slip primer; (4) waterborne inorganic zinc-rich coating; (5) a commonly used complete multi-layer protective coating system; and (6) cold galvanizing. Among these, only treatments (1) and (4) are currently covered by existing standards [6–10], while the other four are not. Based on experimentally determined slip factors, this paper compares recommended values across different codes for surfaces within standard coverage and, for treatments not included in standards, proposes design and code-applicability recommendations grounded in the test results.

The present study provides a systematic experimental calibration of slip factors for six representative faying-surface treatments, including several coating systems not yet covered by current design standards. The results quantitatively reveal the severe degradation of slip resistance induced by thick organic coating systems and, based on two-way analysis of variance (ANOVA), statistically verify that bolt diameter has no significant influence on slip factor within the investigated range. These findings provide direct experimental evidence to improve slip-factor classifications and refine code provisions for coated slip-critical high-strength bolted connections.

2. Slip Factors in High-Strength Bolted Connections

2.1. Influencing Factors of Slip Factors in Coated Faying Surfaces

Existing studies show that the slip factor of high-strength bolted friction-type connections is governed by several key parameters:

(1) Surface roughness—Higher roughness enhances mechanical interlocking and frictional resistance between the faying surfaces, typically achieved through sand-blasting or shot blasting [9].
(2) Surface cleanliness—Contaminants such as oil, dust, or corrosion products significantly reduce friction performance; thus, faying surfaces must be thoroughly cleaned before assembly [9].
(3) Coating type and quality—Different coatings (e.g., epoxy, zinc-rich, polyurethane) exert varying effects on slip resistance. Uniformity and dry film thickness are critical factors [6,9,10], and performance is strongly linked to adhesion between the coating and the substrate [6].
(4) Environmental conditions—Temperature, humidity, and exposure to corrosive media alter coating behaviour and interfacial frictional characteristics [26].
(5) Material properties—The hardness and elastic modulus of the connected components influence micromechanical frictional behaviour [14,20].
(6) Loading conditions—Under long-term or cyclic loading, progressive wear or micro-slip may occur at the interface, reducing the slip factor over time [25].
(7) Construction quality—The control of bolt pretension, surface preparation, and assembly quality also has significant impacts on slip performance [17].

In summary, the slip factor of coated faying surfaces is affected by multiple interacting mechanisms. The frictional behaviour introduced by coatings is complex and remains a major challenge for establishing standardized design provisions.

2.2. Slip Factors in Design Codes and Standards

To regulate the use of slip factors in structural design, many national and regional codes provide recommended values or testing requirements for typical faying surface conditions. Notable standards include JGJ 82-2011 [6], JTG D64-2015 [7], GB 50017-2017 [8], BS EN 1090-2:2018 [9], and ANSI/AISC 360-22 [10]. A summary of their provisions is presented in Table 1. In Table 1, "—" indicates that the corresponding standard does not explicitly specify a slip factor for this surface treatment. All slip-factor values listed are recommended values; the actual design slip factor should be determined comprehensively based on the specific surface-treatment process, construction quality, and relevant test data. Some standards differentiate values by steel grade (e.g., Q235, Q355, Q420); these distinctions have been simplified in this table.

Table 1. Slip factor values are specified in design codes and standards.

Faying Surface Treatment Methods	JGJ 82-2011	JTG D64-2015	GB 50017-2017	BS EN 1090-2:2018	ANSI/AISC 360-22
Sand-blasted/Shot-blasted surface (uncoated)	μ = 0.45	μ = 0.45	μ = 0.40~0.45 (steel-dependent)	Class A: μ = 0.50	Class A: μ = 0.30 Class B: μ = 0.50
Lightly rusted sand-blasted surface	μ = 0.50 (Q355 and above)	—	—	—	—
Hot-dip galvanized surface with sweep blasting.	—	—	—	Class C: μ = 0.35	—
Wire-brushed surface/Clean rolled surface	μ = 0.30~0.40	—	μ = 0.30~0.40 (steel-dependent)	Class C: μ = 0.30	—
Inorganic zinc-rich coating (60–80 μm)	μ = 0.35~0.40	μ = 0.40~0.45	—	Class B: μ = 0.40 (certain coatings)	Class A: μ = 0.30 (certain coatings)
Zinc-rich paint (ZINGA System)	μ = 0.45	μ = 0.45	—	—	—
Zinc silicate coating	μ = 0.40~0.45	μ = 0.35	—	—	—
Thermal-sprayed aluminum/zinc coating (≤80 μm)	—	μ = 0.45	—	Class B: μ = 0.40	—
Primer-only (Anticorrosive base coating)	μ = 0.25	μ = 0.25	—	—	—
Cold-rolled/Rust-affected hot-rolled surface	μ = 0.20~0.25	—	—	Class D: μ = 0.20	—

2.3. Comparative Analysis of Code Provisions on Slip Factors

Although current codes provide systematic guidance on slip factors, substantial differences remain in classification systems, recommended values, and applicability, reflecting varying engineering practices and design philosophies across regions.

To begin with, ANSI/AISC 360-22 classifies faying surfaces into Class A and Class B, corresponding to slip factors of $\mu = 0.30$ and $\mu = 0.50$, respectively, with Class B requiring enhanced roughness and high-quality surface treatment. In contrast, BS EN 1090-2:2018 introduces a more detailed classification system from Class A to Class D, clearly linking surface treatment methods (such as sand-blasting, thermal spraying, wire-brushed, and galvanizing) to slip factor ranges of $\mu = 0.20$–0.50, thereby representing a more systematic European approach.

Chinese standards such as JGJ 82-2011 and GB 50017-2017 adopt a classification framework aligned with practical engineering conditions, combining steel grade and treatment method. For example, sand-blasted surfaces typically use $\mu = 0.45$, while wire-brushed or non-roughened-rolled surfaces use $\mu = 0.30$–0.40, depending on steel strength, highlighting the material dependence of frictional performance.

For coated faying surfaces, discrepancies among standards become even more pronounced. JGJ 82-2011 specifies recommended slip factors for several coating systems—for instance, $\mu = 0.45$ for zinc-rich primers (ZINGA), $\mu = 0.35$–0.40 for inorganic zinc-rich coatings, and as low as $\mu = 0.15$ for polyurethane systems—demonstrating the significant influence of coating type and thickness. In contrast, JTG D64-2015 simplifies the provisions by adopting $\mu = 0.45$ for some coating categories, emphasizing a balance between corrosion protection and mechanical performance in bridge engineering applications.

Furthermore, different codes adopt different approaches to validating surface treatment procedures. ANSI/AISC 360-22 and BS EN 1090-2:2018 explicitly allow slip factors to be determined through testing, whereas JGJ 82-2011—although providing tabulated values—also states that any alternative surface treatment must be verified through experimental testing.

Overall, international standards place greater emphasis on systematic control of surface roughness, treatment procedures, and verification testing, whereas Chinese standards emphasize steel-grade applicability and accumulated engineering practice. Bridge-specific Chinese codes also tend to favour coating systems that provide both corrosion resistance and acceptable slip resistance.

It is noteworthy that the recommended slip factors vary considerably across standards. For example, for sand-blasted (uncoated) faying surfaces, ANSI/AISC 360-22 adopts a more conservative Class B value of $\mu = 0.30$, while the Chinese standards JGJ 82-2011 and JTG D64-2015 specify a higher value of $\mu = 0.45$, which may lead to less conservative predictions of slip resistance. These discrepancies indicate that differences in reliability targets, design assumptions, and application scenarios across countries or regions can lead to significant variations in the slip-factor values recommended for identical or similar surface treatments.

Therefore, for newly introduced surface treatments or coating systems that fall outside the coverage of existing specifications, standardized slip-factor calibration testing remains essential to ensure the safety and reliability of friction-type bolted connections in engineering practice.

3. Slip-Factor Calibration Tests and Results

3.1. Faying-Surface Classification and Preparation

3.1.1. Classification and Arrangement of Faying Surfaces

To systematically evaluate the influence of different faying-surface treatment methods on the slip performance of high-strength bolted connections, six representative surface con-

ditions were selected for comparative slip-factor testing. The objective was to obtain reliable slip-resistance parameters for various treated surfaces, thereby providing reference values for structural design involving new coating systems or combined surface-treatment processes. The experimentally obtained slip factors were further compared with recommended values in current national and international standards to assess their applicability.

Six faying surface treatment methods were adopted in this study:

(1) W-series specimens: sand-blasted faying surfaces, prepared to meet the standard roughness level Sa 2.5;
(2) C-series specimens: faying surfaces coated with an epoxy zinc-rich primer;
(3) S-series specimens: faying surfaces coated with an alcohol-soluble inorganic anti-corrosion anti-slip primer;
(4) series specimens: faying surfaces coated with a waterborne inorganic zinc-rich coating;
(5) X-series specimens: faying surfaces coated with a complete multi-layer protective coating system (epoxy zinc-rich primer + epoxy micaceous iron oxide intermediate coat + acrylic polyurethane topcoat);
(6) D-series specimens: cold-galvanized faying surfaces.

The coating application on the faying surfaces and the measurement of coating thickness are illustrated in Figure 1.

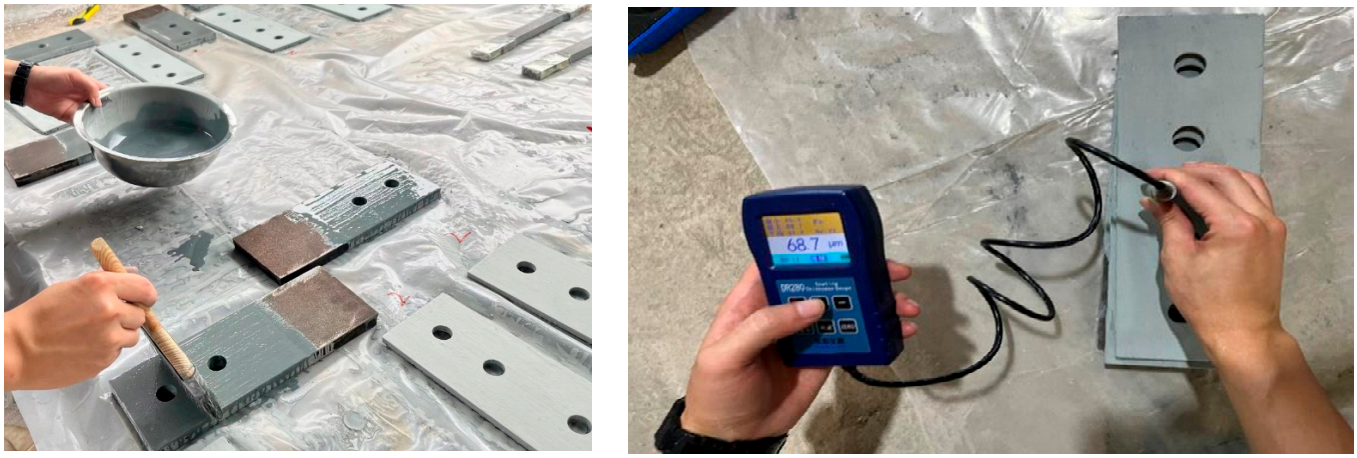


Figure 1. Coating application on the friction surfaces and measurement of coating thickness: (**a**) coating application; (**b**) coating thickness measurement.

Photographs of the six treated faying surfaces are shown in Figure 2.

For consistency and ease of identification, specimen labels follow a unified coding system:

(1) The initial letters W, C, S, A, X, and D correspond to the six faying-surface treatment types;
(2) The middle number denotes the nominal bolt diameter (M20, M18, M16, M12);
(3) The suffixes "−1", "−2", and "−3" represent the three parallel specimens within each group.

Considering practical constraints in testing resources and time, the arrangement of specimens was as follows:

(1) W (sand-blasted), C (epoxy zinc-rich primer), and S (alcohol-soluble inorganic anti-slip primer) treatments were tested for all four bolt diameters (M20, M18, M16, M12);
(2) X (complete multi-layer coating system) specimens were prepared only for M16 bolts;
(3) A (waterborne inorganic zinc-rich coating) and D (cold-galvanized surface) specimens were each prepared only for M12 bolts.

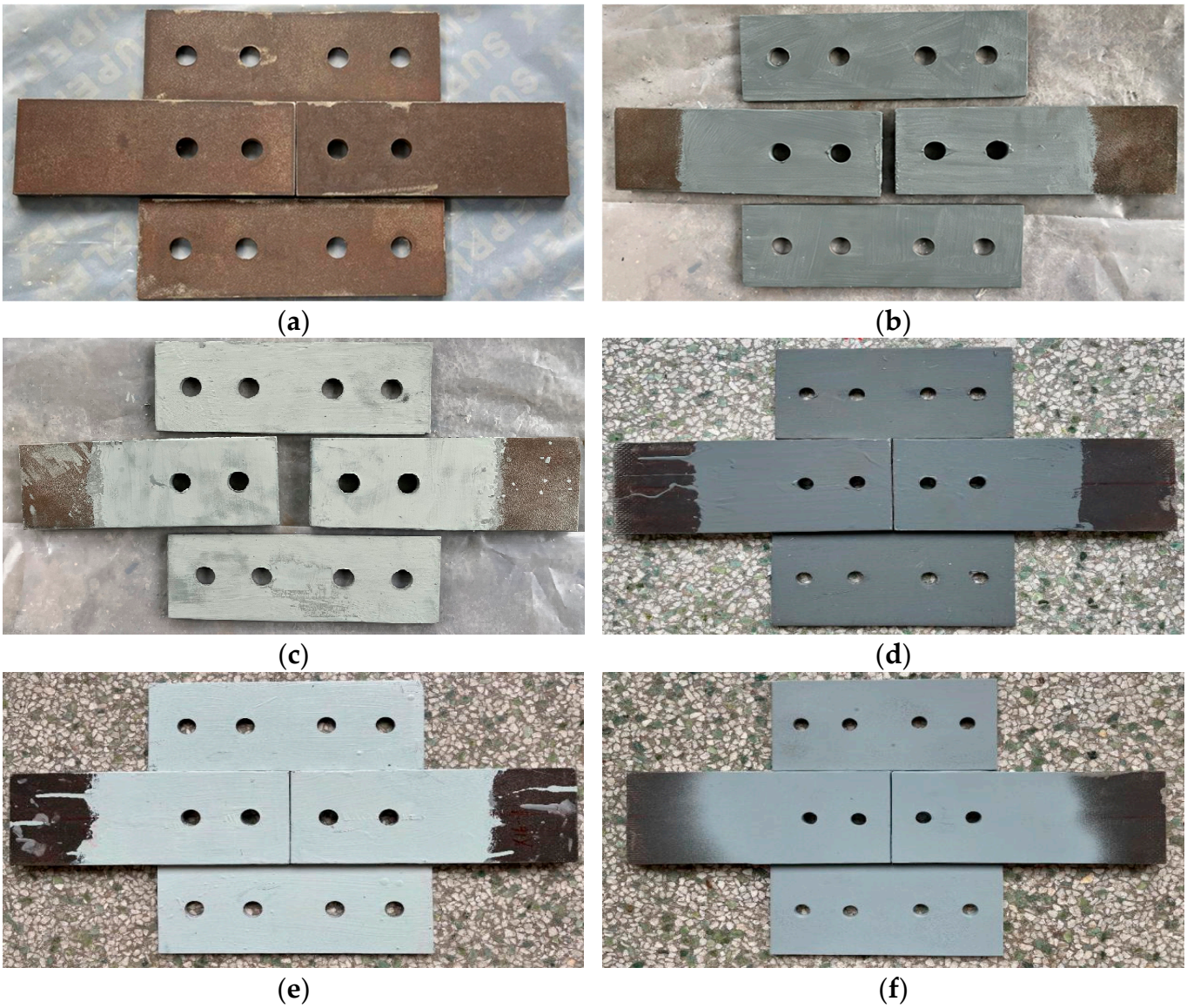


Figure 2. Specimens with six different faying-surface treatment methods. (**a**) W specimen, (**b**) C specimen, (**c**) S specimen, (**d**) A specimen, (**e**) X specimen, (**f**) D specimen.

Among the six investigated faying-surface conditions, the sand-blasted uncoated surface (W type) and the inorganic zinc-rich primer systems (S and A types) correspond to surface categories explicitly covered by existing design codes, and the present tests therefore serve as a calibration-oriented verification of the recommended slip factors. In contrast, the epoxy zinc-rich coating (C type), the thick multi-layer organic coating system (X type), and the cold galvanizing coating (D type) are not explicitly included in current code tables and were selected to represent typical non-standard but realistic engineering scenarios. The C-type coating was chosen because the epoxy zinc-rich primer is currently one of the most widely used and cost-effective anticorrosive coatings permitted for use on faying surfaces according to the design standard [5]. The X-type system was introduced to simulate cases where the entire protective coating system is mistakenly applied to the faying surfaces during construction. The D-type coating was selected to represent rapid field-repair conditions following local coating damage, owing to its short curing time. Consequently, the present test programme provides both code calibration for standard surfaces and experimental evidence for non-standard coated faying surfaces encountered in practice.

3.1.2. Surface Preparation and Coating Application

All coated faying surfaces in this study were prepared by manual brushing, in accordance with the standard application procedures recommended by the coating manufacturers for these products. All coated faying surfaces were prepared in accordance with the surface cleanliness requirement of Sa 2.5 specified in ISO 8501-1 [27] before coating application. Dry abrasive blasting was used to remove mill scale and rust, and all coating operations were carried out in a dry, well-ventilated, and clean workshop environment to ensure construction quality in compliance with the relevant standards [5].

Before coating application and specimen assembly, all steel plates were inspected for out-of-plane deformation and surface flatness using a straightedge and feeler gauges. Only plates meeting the workshop flatness quality-control requirements were accepted, ensuring that slip performance was not affected by unintended plate deformation.

According to the roughness classification specified in ISO 8503-2 [28], blasted surfaces are classified as having a medium surface profile, with a typical peak-to-valley height (Rz) of 50–90 μm. This level of surface roughness is generally considered suitable for the application of zinc-rich anticorrosive primers with a dry film thickness greater than 45 μm, as it provides an appropriate balance between mechanical interlocking and coating adhesion. Previous studies have demonstrated that a medium surface roughness is critical for both the adhesion performance and corrosion-protection efficiency of zinc-rich coatings on steel substrates [29].

The C-type epoxy zinc-rich primer was a two-component system (Components A and B) with a nominal zinc content of approximately 70%. Component A consisted of epoxy resin, curing agent, zinc powder, and organic solvent, while Component B was a polyamide curing agent. After mixing, the effective pot life was about 5 h. The coating was applied by brush coating on Sa 2.5 blast-cleaned steel surfaces, with the dry film thickness controlled at 110–120 μm. The nominal curing time was 72 h, while in the present study, all C-type specimens were cured for more than 7 days before slip testing.

The S-type alcohol-soluble inorganic anticorrosive anti-slip primer was a three-component system with a mass ratio of A (paste):B (main agent):C (powder) = 1:3:16. The detailed chemical composition is proprietary and therefore not disclosed. After mixing, the effective pot life was approximately 6 h. The coating was applied by brush on Sa 2.5 blast-cleaned surfaces, with the dry film thickness controlled at 80–100 μm. The nominal curing time was 7 days, and all S-type specimens in the present study were cured for more than 7 days before testing.

The A-type waterborne inorganic zinc-rich coating was also a two-component system with a nominal zinc content of about 70%. Component A consisted of a waterborne epoxy resin emulsion, deionized water, zinc powder, and additives, while Component B was a waterborne amine curing agent. After mixing, the effective pot life was approximately 5 h. The coating was applied by brush on Sa 2.5 blast-cleaned surfaces, with the dry film thickness controlled at 90–100 μm. The nominal curing time was 72 h, and all A-type specimens used in the present tests were cured for more than 7 days.

The X-type complete multi-layer coating system comprised an epoxy zinc-rich primer (≈80 μm), an epoxy micaceous iron oxide intermediate coat (≈80 μm), and an acrylic polyurethane topcoat (≈80 μm), resulting in a total dry film thickness of approximately 240–250 μm. All layers were applied by brush on the Sa 2.5 blast-cleaned steel surfaces. The epoxy zinc-rich primer was identical in composition and application procedure to that used for the C-type specimens. The epoxy micaceous iron oxide intermediate coat was also a two-component system, with Component A comprising epoxy resin, a curing agent, micaceous iron oxide, and an organic solvent, and Component B comprising a polyamide curing agent. After mixing, the effective pot life was about 5 h, and the intermediate

coat was applied 24 h after the primer had cured. The acrylic polyurethane topcoat was likewise a two-component system comprising a hydroxyl-acrylic resin (Component A) and an aliphatic polyurethane curing agent (Component B). It was applied 24 h after the intermediate coat, with a nominal curing time of 36 h. All X-type specimens in this study were cured for more than 7 days before testing.

D-type cold galvanizing coating was a single-component, heavy-duty anticorrosive coating composed mainly of zinc powder (purity > 99.9%), a special resin, a volatile solvent, additives, and a propellant, and was supplied in aerosol packaging via high-pressure filling. The total zinc content of the coating exceeded 96%, and the zinc content in the dry film exceeded 95%. The coating was applied by spray coating, with the dry film thickness controlled at 80–90 μm. The nominal curing time was 24 h, and all D-type specimens in this study were cured for more than 24 h before testing.

All coating applications were carried out under controlled indoor environmental conditions. During application and curing, the workshop temperature was maintained at approximately 15–25 °C, and the relative humidity was kept below 70%, satisfying the manufacturers' recommended ranges and preventing adverse effects such as incomplete curing, condensation, or surface defects. All specimens were cured for durations longer than the nominal minimum curing times to eliminate potential environmental variability and ensure consistent coating quality.

Overall, the coating application environment during the present experimental programme was kept dry, clean, and well ventilated, ensuring that the construction quality of all coating systems satisfied the relevant standard requirements [5].

3.2. Slip-Factor Testing Method

Under standard loading conditions [6], bolted connection specimens with different faying-surface treatments were prepared and subjected to static tensile loading to determine the critical slip load, from which the slip factor was calculated. For each surface-treatment type, three parallel specimens were tested to ensure data stability and repeatability. The measured coating thicknesses for all specimens are listed in Table 2.

The connection steel plates were fabricated from Q355B structural steel with a nominal yield strength of 355 MPa. The core plate was 16 mm thick, while the cover plates were 8 mm thick. All high-strength bolts used in the tests were of property class 8.8. The nominal bolt diameters were M20, M18, M16, and M12, with corresponding applied pretension forces P of 125 kN, 100 kN, 80 kN, and 45 kN, respectively. All bolts were tightened using a calibrated torque wrench based on a pre-established torque–pretension relationship obtained from a bolt tension calibrator, ensuring consistent preload among all specimens.

The present study is purely experimental in nature and does not involve any numerical or theoretical benchmark model. The slip factor was calculated in accordance with the provisions of JGJ 82-2011 [6], using the standard definition adopted in this code. In the present double-lap joint configuration, the slip factor is defined as the ratio between the measured slip load at the onset of macroscopic slip and the effective normal force generated by bolt pretension. The standard equation of slip factor is $\mu = F/N$, where F is the measured slip load at the onset of macroscopic slip, and $N = n_f \sum_{i=1}^{m} P_i$. n_f is the number of faying surfaces, taken as $n_f = 2$ in this test; $\sum_{i=1}^{m} P_i$ is the total bolt pretension force, with $m = 2$ in this test. The calculation equation definition fully follows the testing methodology specified in JGJ 82-2011, and no additional assumptions or modified formulations are introduced.

Table 2. Specimen Identifications and Measured Data.

Specimen ID	Bolt	Coating Thickness of Faying Surface (μm)	F (kN)	N (kN)	Slip Factor	Slip Factor (Average)	SD	COV
W20-1	M20	0	226.04	500	0.45	0.45	0.03	0.06
W20-2			234.85	500	0.47			
W20-3			210.75	500	0.42			
W18-1	M18		182.2	400	0.46	0.43	0.03	0.07
W18-2			158.45	400	0.40			
W18-3			176.39	400	0.44			
W16-1	M16		135.67	320	0.42	0.44	0.02	0.05
W16-2			147.01	320	0.46			
W16-3			139.09	320	0.43			
W12-1	M12		84.25	180	0.47	0.45	0.02	0.05
W12-2			78.26	180	0.43			
W12-3			79.78	180	0.44			
S20-1	M20	92.85	252.15	500	0.50	0.49	0.01	0.01
S20-2		90.84	247.2	500	0.49			
S20-3		95.67	243.45	500	0.49			
S18-1	M18	89.73	197.78	400	0.49	0.51	0.02	0.03
S18-2		96.26	206.75	400	0.52			
S18-3		92.44	203.8	400	0.51			
S16-1	M16	92.28	151.34	320	0.47	0.49	0.02	0.03
S16-2		92.36	156.75	320	0.49			
S16-3		90.73	158.78	320	0.50			
S12-1	M12	92.66	89.61	180	0.50	0.51	0.03	0.06
S12-2		86.43	86.9	180	0.48			
S12-3		88.60	96.34	180	0.54			
C20-1	M20	113.84	149.97	500	0.30	0.28	0.02	0.07
C20-2		110.75	138	500	0.28			
C20-3		109.63	129.71	500	0.26			
C18-1	M18	116.43	98.48	400	0.25	0.26	0.01	0.04
C18-2		113.40	106.65	400	0.27			
C18-3		108.49	105	400	0.26			
C16-1	M16	112.46	97.77	320	0.31	0.28	0.03	0.11
C16-2		114.73	81.2	320	0.25			
C16-3		110.71	91.5	320	0.29			
C12-1	M12	106.82	49.63	180	0.28	0.27	0.03	0.11
C12-2		114.90	54.28	180	0.30			
C12-3		115.37	43.93	180	0.24			
X16-1	M16	234.39	78.52	320	0.25	0.23	0.02	0.07
X16-2		246.80	69.43	320	0.22			
X16-3		251.77	73.76	320	0.23			
A12-1	M12	100.58	58.67	180	0.33	0.33	0.01	0.03
A12-2		103.81	58.21	180	0.32			
A12-3		96.83	61.28	180	0.34			
D12-1		85.39	77.38	180	0.43	0.44	0.01	0.03
D12-2		79.10	77.74	180	0.43			
D12-3		89.66	80.26	180	0.45			

Slip-factor tests were conducted using a 200 t electro-hydraulic servo universal testing machine. Two electronic displacement transducers were installed to measure the relative slip between the faying surfaces (Figure 3). The loading protocol consisted of two stages: (1) displacement-controlled loading at 2 mm/min to 10% of the design slip load, followed by a 1 min hold to ensure system stability; and (2) continued loading at the same rate until macroscopic slip occurred. At the slip point, the load was held for an additional minute to confirm proper operation of the testing machine and measurement devices.

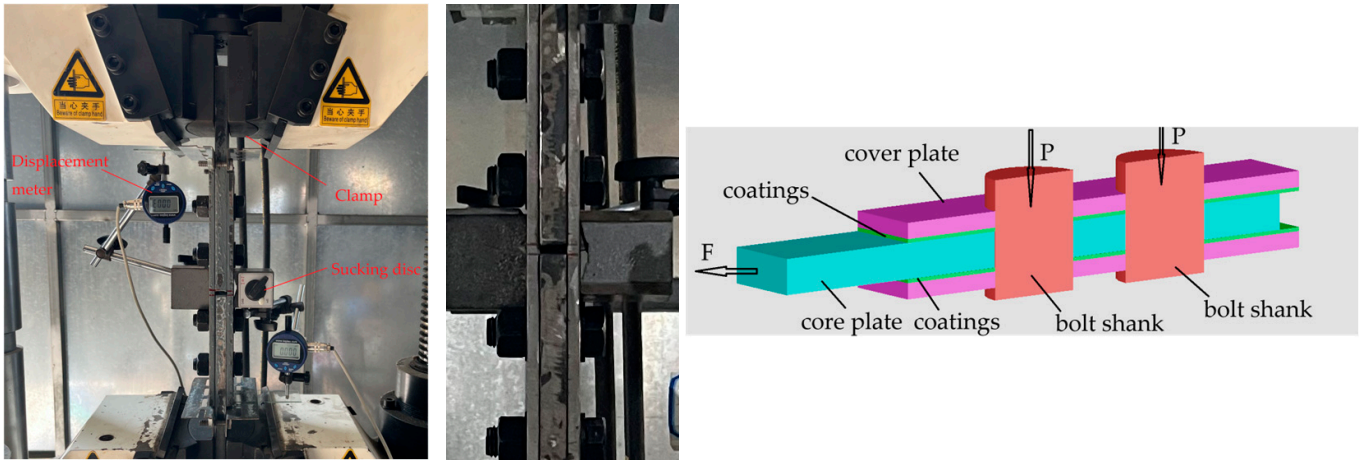


Figure 3. The specimen is under shear testing. (**a**) Testing setup, (**b**) specimen after slipping, (**c**) force transfer and friction mechanism at coated faying surfaces.

As shown in Figure 3a, all slip-factor tests were performed within one hour after bolt installation, during which any potential loss of bolt pretension is generally negligible for high-strength bolts. Even if minor relaxation were to occur, using the nominal pretension value would still result in a slightly conservative, lower-bound estimate of the slip factor. Slip failure was identified by a sudden increase in measured slip displacement accompanied by a distinct drop in the force–displacement response. An example of this characteristic behaviour is shown in Figure 3b.

As illustrated in Figure 3c, the load transfer mechanism in the present slip-factor tests is governed by frictional resistance developed at the coated faying surfaces under bolt pretension. The applied bolt pretension P generates a normal compressive force acting on each faying surface, while the externally applied tensile load is resisted by the friction force F mobilized at the interfaces between the cover plates and the core plate. In the tested double-lap configuration, frictional resistance develops at the two faying surfaces, and the total slip resistance is the sum of the friction forces acting at each interface.

In this context, the slip factor is the ratio of the measured slip load to the effective normal force generated by bolt pretension. The schematic diagram in Figure 3c is provided to clarify the physical meaning of the forces involved and to illustrate how slip resistance is mobilized through interfacial friction rather than through the bearing action of the bolt shank or the deformation of the connected plates. It should be noted that the present study focuses on the macroscopic force-transfer mechanism relevant to slip-factor calibration, rather than on detailed micro-scale tribological processes at the coating interface.

4. Test Results and Statistical Analysis

4.1. Slip-Factor Test Results and Variability Analysis

Table 2 summarizes the slip-factor test results of all 45 specimens. Based on the experimental data, the statistical indicators for each surface-treatment group, including

the mean slip factor, standard deviation (SD), and coefficient of variation (COV), were calculated to quantitatively evaluate both the average slip resistance and the dispersion of the test results.

The mean slip factors clearly demonstrate that the faying-surface condition and coating type exert a pronounced influence on the slip performance of high-strength bolted connections.

For the sand-blasted, uncoated surfaces (W type), the mean slip factors range from 0.43 to 0.45, with COV values of 0.05 to 0.07, indicating stable frictional performance and good repeatability. This consistency reflects the favourable surface roughness and mechanical interlocking characteristics of abrasive-blasted steel, and the results are relatively uniform across different bolt diameters, supporting the role of W-type surfaces as a benchmark condition in current design standards.

The alcohol-soluble inorganic anti-slip primer surfaces (S type) show the highest slip resistance among all tested surface conditions, with mean slip factors ranging from 0.49 to 0.51 and generally low COV values (mostly below 0.06). The superior slip performance is attributed to the combined effects of good coating adhesion and micro-scale mechanical interlocking while maintaining a relatively rough surface, making this surface condition suitable for applications requiring both high slip resistance and corrosion protection.

In contrast, the epoxy zinc-rich-coated surfaces (C type) result in significantly reduced slip factors, with mean values of 0.26–0.28, accompanied by relatively larger COV values (up to 0.11 for some groups). Although the epoxy zinc-rich coating provides excellent corrosion resistance, its relatively smooth polymeric binder matrix and larger dry-film thickness introduce a partial lubricating effect at the interface, thereby diminishing the interfacial frictional resistance.

The waterborne inorganic zinc-rich coating (A type) exhibits moderate slip resistance, with a mean slip factor of approximately 0.33, indicating that this surface condition is suitable for engineering applications where moderate corrosion protection is required but high slip resistance is not critical.

The thick multi-layer organic coating system (X type) produces the lowest slip resistance, with a mean slip factor of only about 0.23. The substantial total dry film thickness (240–250 μm) significantly reduces the effective surface roughness and mechanical interlocking at the interface, making this system unsuitable for slip-critical joints unless additional surface roughening treatments are applied.

The cold galvanizing coating (D type) demonstrates favourable slip resistance, with a mean slip factor of approximately 0.44, indicating a desirable balance between corrosion protection and interfacial frictional performance after rapid field repair.

Overall, the SD values across all surface-treatment groups range from 0.006 to 0.031, and the corresponding COV values are generally less than 0.11, indicating acceptable data dispersion and satisfactory repeatability of the slip-factor tests. These results confirm that the slip resistance of friction-type bolted connections is primarily governed by the faying-surface treatment, rather than by random experimental scatter.

4.2. Statistical Significance Analysis Based on One-Way ANOVA

To further evaluate the statistical significance of the influence of different faying-surface treatments on the slip factor, a one-way analysis of variance (ANOVA) was performed following the standard statistical procedure described by Montgomery [30]. Because the number of tested specimens differs across surface types, an unbalanced one-way ANOVA was used. The significance level was set to 0.05.

The ANOVA results yield an F value of 210.78 with a corresponding p-value of 4.01×10^{-27}, which is far lower than 0.01. This clearly demonstrates that the type of faying-surface treatment has an extremely significant influence on the slip factor ($p < 0.01$).

The strong statistical significance is consistent with the large differences observed among the mean slip factors of different surface conditions. In particular, inorganic anti-slip primer surfaces (S type) lead to significantly higher slip resistance, whereas epoxy zinc-rich coatings (C type) and thick multi-layer organic systems (X type) cause substantial reductions in slip performance. The ANOVA results, therefore, provide solid statistical support for the reliability of the observed trends and for the subsequent comparative analysis with design code provisions.

4.3. Influence of Bolt Diameter (Two-Way ANOVA)

In addition to surface-treatment effects, the influence of bolt diameter on the slip factor was further examined. For the W-, S-, and C-series specimens, a two-way analysis of variance (ANOVA) with replication was conducted by considering the surface-treatment type (W, S, C) and bolt diameter (M12, M16, M18, and M20) as two independent factors, following the standard procedure described by Montgomery [30].

The results show that the surface-treatment type has an extremely significant main effect ($p < 0.01$), whereas the main effect of bolt diameter is not statistically significant ($p > 0.5$). In addition, the interaction effect between surface-treatment type and bolt diameter is also statistically insignificant.

Although a numerical variation of approximately 5%–8% in the slip factor can be observed among different bolt diameters, the ANOVA results demonstrate that this variation is not statistically meaningful and remains secondary compared with the dominant influence of the faying-surface condition.

From a mechanical perspective, the minor influence of bolt diameter can be attributed to the fact that slip resistance is primarily governed by the macroscopic normal force generated by bolt pretension and the tribological characteristics of the faying surfaces. In contrast, variations in bolt diameter mainly affect the local contact pressure distribution and bearing conditions near the bolt holes. These local effects result in only limited changes in slip behaviour and therefore do not govern the overall slip resistance.

4.4. Failure Modes and Post-Slip Surface Characteristics

During the slip-factor tests, the load–displacement responses of all specimens were continuously monitored until macroscopic slip occurred, and a stable sliding phase was reached. Since the purpose of this study was to determine slip coefficients rather than ultimate capacity, the tests were terminated after stable sliding, and no bearing failure, bolt fracture, or plate tearing was observed. Thus, all specimens failed solely due to interfacial slip. Only the peak slip loads and the corresponding post-slip faying-surface morphologies are analyzed here.

Representative post-slip surface characteristics of the six surface-treatment types are shown in Figure 4. All specimens exhibit clear frictional wear marks, confirming that sliding occurred at the steel–coating or coating–coating interface. The degree and pattern of wear provide important physical insights into the friction mechanisms governing the measured slip factors.

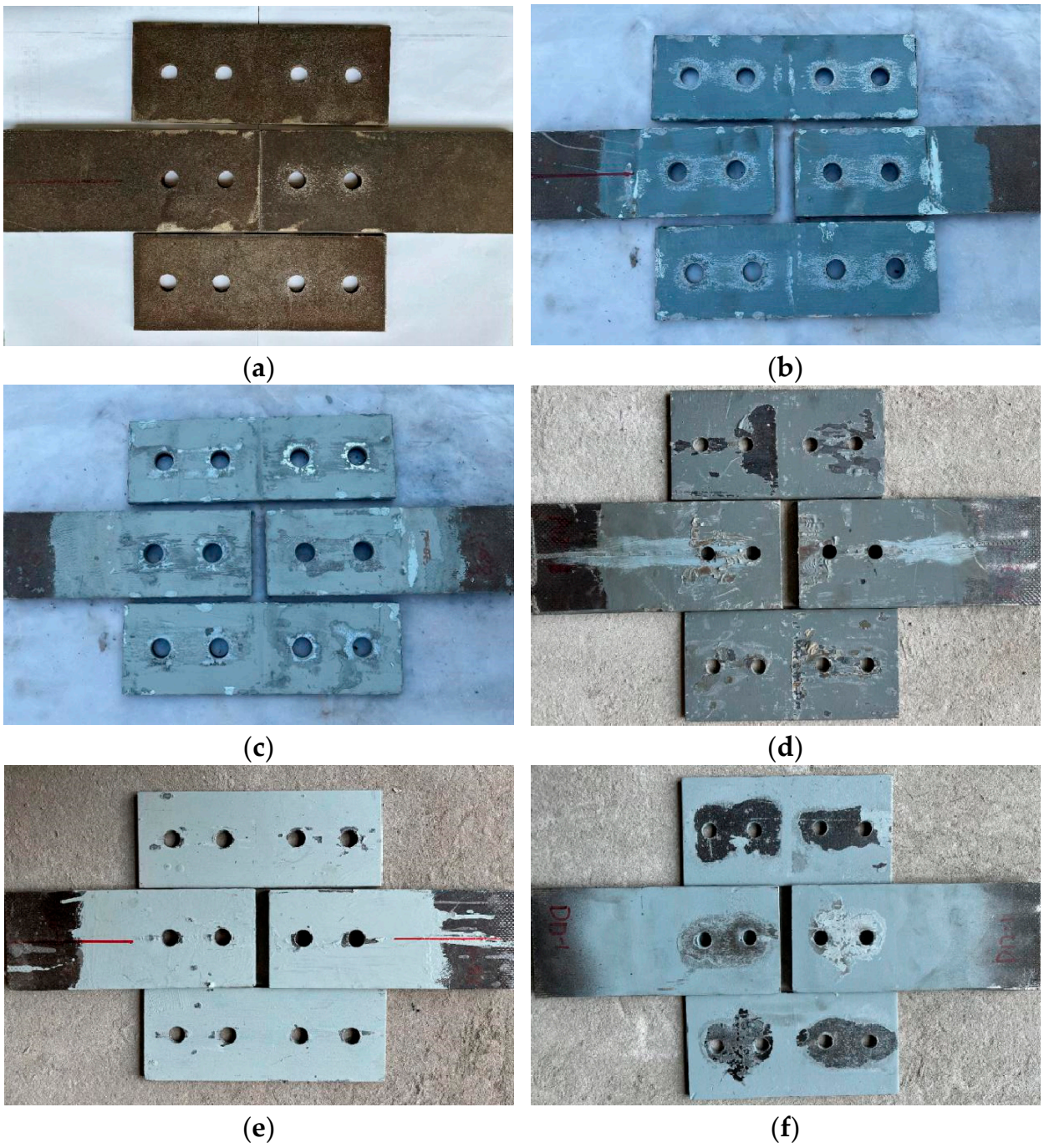


Figure 4. Post-slip faying-surface morphologies of high-strength bolted specimens with different surface treatments. (**a**) W specimen [3] (approved by the copyright holder.), (**b**) C specimen [3] (approved by the copyright holder.), (**c**) S specimen [3] (approved by the copyright holder.), (**d**) A specimen, (**e**) X specimen, (**f**) D specimen.

(1) Sand-blasted surfaces (W type)

Whitening and polishing around bolt holes indicate extensive asperity shearing and hard–hard contact. The dense distribution of micro-ploughing marks indicates that mechanical interlocking was the dominant friction mechanism, consistent with the high, stable slip factors (μ = 0.43–0.45).

(2) Epoxy zinc-rich primer (C type)

Friction marks appeared around bolt holes, between hole pairs, and along plate edges. However, the coating film remained largely intact, with no visible spallation. This indicates that slip was primarily accommodated by shear deformation within the polymer matrix rather than substrate interlocking. Because epoxy forms a relatively smooth, continuous film with lower shear resistance, the friction mechanism is governed by coating shear rather than metal–metal asperity engagement, explaining the reduced slip factors (μ = 0.26–0.28).

(3) Alcohol-soluble inorganic anti-slip primer (S type)

Wear traces were distributed over the entire faying surface, with pronounced whitening near bolt holes. The coating remained well bonded after slip, indicating a hybrid friction mechanism: (i) micro-shear within the inorganic matrix and (ii) partial substrate asperity engagement due to the rougher cured surface. This dual mechanism explains why S-type coatings exhibited the highest slip factors (μ = 0.49–0.51) among all tested surfaces.

(4) Waterborne inorganic zinc-rich coating (A type)

Distinct frictional wear and partial coating removal were observed, especially around bolt holes. The local exposure of the steel substrate suggests that the coating underwent moderate brittle fracture during sliding. Because the cured film is harder but less ductile than organic coatings, interfacial cracking reduces real contact area and effective mechanical interlocking, resulting in moderate slip resistance ($\mu \approx 0.33$).

(5) Multi-layer coating system (X type)

Wear marks were concentrated around bolt holes, accompanied by evident coating delamination and layer separation. Slip likely occurred either at the coating–substrate boundary or within the interlayer interfaces, both of which possess low shear strength. The thick organic film (≈240–250 μm) further suppresses steel–steel contact, explaining the extremely low slip factor ($\mu \approx 0.23$).

(6) Cold-galvanized surfaces (D type)

Extensive polishing and zinc-layer removal were observed near bolt holes. The sacrificial zinc film exhibited abrasive wear, exposing localized metal-to-metal contact that enhanced frictional interlocking. This mechanism aligns with the favourable slip performance ($\mu \approx 0.44$), which is slightly higher than that of typical zinc-based coatings.

Across all surface types, the observed slip behaviour is governed by three competing mechanisms: (1) mechanical interlocking of steel asperities; (2) shear deformation or fracture of coating films; (3) interfacial debonding or interlayer sliding. Surfaces that maintain hard–hard asperity interlocking (W and D types) exhibit higher slip factors, whereas surfaces dominated by polymeric shear (C type) or interlayer sliding (X type) show markedly reduced friction resistance. The S-type coating provides an optimal combination of interlocking and coating shear resistance, resulting in the highest slip factors.

A detailed microscopic characterization (SEM, 3D profilometry) to quantify coating damage and asperity degradation will be included in future work.

5. Applicability Analysis of Code-Recommended Slip Factors

Based on the slip factors obtained from the experimental programme and the recommended values in major domestic and international design standards, the applicability, compliance, and potential deviations of each faying-surface treatment are evaluated in terms of engineering design implications, as follows.

5.1. Sand-Blasted Surfaces (W Type)

This surface condition is uncoated and provides a high and stable level of surface roughness. The measured slip factors range from 0.43 to 0.45, with low variability, and show excellent agreement with the value of $\mu = 0.45$ specified in JGJ 82-2011, JTG D64-2015, and GB 50017-2017. This confirms that the current Chinese provisions are appropriate and neither overly conservative nor unconservative for sand-blasted faying surfaces.

In contrast, ANSI/AISC 360-22 adopts a lower value of $\mu = 0.30$, indicating a more conservative design approach for this surface condition. According to the classification systems of ANSI/AISC 360-22 and BS EN 1090-2:2018, the present sand-blasted surfaces can be classified as Class B, offering reliable slip-critical performance. Therefore, W-type surfaces may be regarded as a benchmark reference condition for both engineering design and experimental calibration.

5.2. Alcohol-Soluble Inorganic Anti-Corrosion Anti-Slip Primer (S Type)

The alcohol-soluble inorganic anti-corrosion anti-slip primer exhibited the highest slip resistance among all investigated surface conditions, with measured slip factors ranging from $\mu = 0.49$ to 0.51, which are even higher than those of sand-blasted surfaces. This indicates that the S-type coating not only provides effective corrosion protection but also preserves a high level of interfacial frictional resistance.

Although this coating type is not yet explicitly included in current Chinese design standards, its excellent slip performance suggests that adopting existing Class A or Class B provisions would yield conservative estimates of slip resistance. From the perspective of international classification systems, the S-type surface condition is consistent with Class B or above performance. The present experimental results, therefore, provide quantitative evidence for establishing an independent classification or assigning a higher recommended design slip factor of approximately $\mu = 0.50$ for this coating system in future revisions of design codes.

From a practical engineering viewpoint, this surface treatment shows strong potential for slip-critical connections that require both high slip resistance and enhanced corrosion durability, making it particularly attractive for applications in aggressive service environments.

5.3. Epoxy Zinc-Rich Primer (C Type)

As widely used corrosion-protection systems, epoxy zinc-rich primers yielded relatively low slip factors of 0.26–0.28, which are significantly lower than those of sand-blasted surfaces. This reduction is mainly attributed to the dense and relatively smooth polymeric coating film, which weakens mechanical interlocking at the faying interface.

These values fall below the lower bound of Class A surfaces ($\mu = 0.30$) specified in most domestic and international standards. If this coating type is treated as a conventional friction surface in design, the direct adoption of standard Class A values would result in a systematic overestimation of slip resistance and potential safety risks. Therefore, epoxy zinc-rich primers should either be assigned a lower slip classification or be combined with additional roughening treatments when used in slip-critical joints. A conservative design range of $\mu = 0.25$–0.28 is recommended.

From a mechanistic viewpoint, the reduced slip performance of the C-type coating results from several coupled factors. After curing, the epoxy binder forms a smooth, continuous surface film that suppresses micro-scale asperity interlocking, which normally governs frictional resistance on uncoated or roughened steel surfaces. Meanwhile, the cross-linking and densification of the epoxy matrix during curing produce a hard but relatively low-shear-strength interfacial layer, which is prone to interfacial shear sliding

under high contact pressure. Moreover, although the coating contains a high fraction of zinc particles, they are largely embedded in a continuous resin matrix and do not significantly enhance friction unless they are sufficiently exposed to form direct metallic contact points.

From an engineering perspective, the slip resistance of epoxy zinc-rich coatings can be improved through appropriate surface modification and pre-treatment measures, such as:

(i) Sweep blasting or light re-blasting of the cured coating to reintroduce surface roughness;
(ii) Reducing the total dry-film thickness to mitigate the lubricating effect of the resin-rich surface layer;
(iii) Introducing rough inorganic fillers or anti-slip aggregates into the coating formulation.

These measures are expected to enhance mechanical interlocking while maintaining adequate corrosion protection.

5.4. Complete Multi-Layer Coating System (X Type)

The complete multi-layer protective coating system produced the lowest slip resistance, with a mean slip factor of only $\mu \approx 0.23$. The smooth surface texture and the excessive total dry-film thickness markedly reduce both surface roughness and mechanical interlocking, resulting in a severe degradation of frictional resistance.

According to the classification systems of BS EN 1090-2:2018 and ANSI/AISC 360-22, this surface condition does not fall within any existing Class A or Class B category and should therefore be treated as a non-friction-type surface. From a design safety perspective, treating such a surface as a conventional friction surface would be highly unconservative. It is thus strongly recommended that design specifications explicitly state that complete multi-layer coating systems are not permitted for slip-critical connections. If such a coating is mistakenly applied to a faying surface in engineering practice, it should be removed immediately.

From a mechanistic standpoint, the extremely low slip resistance of the X-type system is mainly due to its multi-layer polymeric nature and excessive total film thickness. The epoxy zinc-rich primer, epoxy micaceous iron oxide intermediate coat, and acrylic polyurethane topcoat together form a thick, compliant, and relatively smooth composite interface, significantly reducing the real contact area between the hard asperities of the steel substrates. Moreover, the organic topcoat exhibits a comparatively low interfacial shear strength, and micro-slip can readily occur either within the coating layers or at the coating–substrate interface.

In addition, the stepwise curing process of the multi-layer system may lead to weak interlayer bonding or local mechanical property heterogeneity, which further promotes interfacial sliding under high normal pressure. As a consequence, such thick multi-layer coating systems are inherently unfavourable for slip-critical connections.

From a practical viewpoint, the slip resistance of such surfaces can only be enhanced through aggressive pre-treatment measures, such as the complete removal of the organic coating at the faying surfaces, followed by re-blasting, or by the local application of dedicated anti-slip inorganic primers before bolt assembly. Direct modification of the complete multi-layer system itself is generally ineffective and economically impractical for improving slip resistance in slip-critical joints.

5.5. Waterborne Inorganic Zinc-Rich Coating (A Type)

The waterborne inorganic zinc-rich coating exhibited moderate slip resistance, with a measured slip factor of $\mu \approx 0.33$. These values are slightly higher than the values of $\mu = 0.30$ recommended in JTG D64-2015 and GB 50017-2017, indicating that the current Chinese provisions are generally conservative for this type of coating.

According to the classification systems of ANSI/AISC 360-22 and BS EN 1090-2:2018, this surface condition corresponds to Class A. From a design standpoint, the A-type coating is suitable for structural applications that require moderate slip performance and corrosion protection, but it is not recommended for highly slip-critical joints.

Based on the current test results, a recommended design range of $\mu = 0.30–0.33$ is considered appropriate for waterborne inorganic zinc-rich-coated faying surfaces.

5.6. Cold-Galvanized Surface (D Type)

The cold-galvanized surfaces demonstrated favourable slip resistance, with a mean slip factor of approximately $\mu \approx 0.44$, which is slightly higher than some existing code recommendations for zinc-based surface treatments (e.g., $\mu = 0.40$ in JTG D64-2015). This improvement is mainly attributed to the surface roughness and mechanical interlocking created by the cold-galvanizing process.

According to international classification systems, this slip resistance level corresponds to Class B surface performance. From a practical engineering perspective, the D-type surface offers a desirable balance between corrosion protection and frictional resistance, particularly for on-site repair or maintenance scenarios where rapid re-coating and a short curing time are required.

Based on the current experimental evidence, a recommended design range of $\mu = 0.40–0.45$ is reasonable for cold-galvanized faying surfaces used in slip-critical or near-slip-critical connections.

Overall, this comparative analysis indicates that current design standards provide reliable guidance for uncoated sand-blasted surfaces and inorganic zinc-rich coatings, but may be non-conservative for epoxy zinc-rich primers and thick multi-layer organic coating systems when applied to faying surfaces. The present experimental results, therefore, offer direct quantitative evidence for refining slip-factor classifications of coated surfaces and provide a valuable technical basis for future revisions of slip-factor provisions by design code committees.

5.7. Comparison with Published International Slip-Factor Data

The slip-factor results obtained in this study are broadly consistent with the trends reported in recent international investigations on coated and uncoated steel faying surfaces.

For uncoated sand-blasted surfaces, the measured slip factors ($\mu = 0.43–0.45$) agree well with the values reported by Annan and Chiza [11,31], who found that properly prepared blasted or metallized/galvanized surfaces can achieve Class B friction performance. This confirms that the Sa 2.5 blasted surfaces in the present study fall within the upper range of internationally reported values for roughened steel interfaces.

For inorganic zinc-rich coatings, the slip factor of approximately $\mu \approx 0.33$ obtained here matches the values reported by Wang et al. [12] for Q345 steel (equivalent to Q355 under the updated Chinese designation system). Their study showed that inorganic zinc-rich primers with coating thicknesses of 60–80 μm typically achieve $\mu \approx 0.30–0.36$, consistent with Class A classification in several international standards and aligning well with our A-type coating results.

For organic zinc-rich coatings, the relatively low slip-factor range of $\mu = 0.26–0.28$ measured for the C-type coating is comparable to the friction levels reported by Collini et al. [17] for galvanized and weathering steel interfaces. Their results similarly demonstrated that smooth or dense coating films tend to suppress asperity interlocking and reduce slip resistance, explaining the similarity in performance.

Higher slip factors reported in certain studies—such as those for metallized surfaces or mechanically roughened galvanized coatings in Annan and Chiza [11,31]—are consistent

with our findings for the S-type coating (μ = 0.49–0.51), which also achieves high friction through a combination of mechanical anchoring and coating microstructure. This alignment further validates the high-performance behaviour observed in the S-type system.

Overall, differences among slip-factor values reported in the literature can be attributed to: (1) variations in surface preparation and resulting roughness; (2) coating chemistry and dry-film thickness; and (3) differences in test procedures, specimen geometry, and preload prescriptions.

As highlighted by Fuente et al. [24], geometric and procedural inconsistencies across national standards alone can cause more than 40% variation in effective friction area and significantly affect slip-factor measurements. These factors explain why nominally similar surface treatments sometimes exhibit noticeable differences in reported friction performance.

6. Conclusions

This study experimentally evaluated the slip factors of high-strength bolted friction-type connections with six representative faying-surface treatment methods, including both coated and uncoated conditions. A total of 45 tensile specimens were tested, and the measured slip factors were systematically compared with the recommended values in major domestic and international design standards. The main conclusions can be drawn as follows:

1. Faying-surface treatment plays a dominant role in governing slip resistance, whereas the influence of bolt diameter is statistically insignificant within the investigated range (M12–M20). Although numerical variations of about 5%–8% are observed across different bolt diameters under the same surface condition, two-way ANOVA confirms that this effect is not statistically significant, supporting the basic assumption adopted in current design codes.
2. Sand-blasted surfaces (W type) provide stable, reliable slip resistance with slip factors μ = 0.43–0.45, which agree well with the values recommended in existing standards (e.g., μ = 0.45 in JGJ 82-2011). Their variation across different bolt diameters is less than ±3%, confirming their role as a benchmark surface condition for slip-critical design.
3. Alcohol-soluble inorganic anti-corrosion anti-slip primer surfaces (S type) exhibit the highest slip resistance among all investigated treatments, with slip factors of μ = 0.49–0.51, representing an increase of approximately 13%–18% compared with sand-blasted surfaces. This surface condition shows strong potential for engineering applications that require both high slip resistance and corrosion resistance.
4. Epoxy zinc-rich primer surfaces (C type) yield relatively low slip factors of μ = 0.26–0.28, corresponding to a 35%–45% reduction relative to sand-blasted surfaces. These values fall below the lower bound of Class A surfaces (μ = 0.30) in most standards, indicating that such coatings will lead to a significant overestimation of slip resistance if treated as conventional friction surfaces and should therefore be used with caution or combined with additional roughening measures in slip-critical joints.
5. Complete multi-layer protective coating systems (X type) exhibit the lowest slip resistance, with a mean value of μ ≈ 0.23, representing a reduction of about 50% compared with sand-blasted surfaces. This severe degradation is attributed to the excessive total dry-film thickness (240–250 μm), which markedly suppresses surface roughness and mechanical interlocking. Such systems are therefore unsuitable for slip-critical applications unless the faying surfaces are fully re-treated.
6. Waterborne inorganic zinc-rich coatings (A type) and cold-galvanized surfaces (D type) provide moderate and favourable slip performance, respectively, with mean values of μ ≈ 0.33 and μ ≈ 0.44. Compared with sand-blasted surfaces, A-type coatings show a reduction of about 25%, whereas D-type surfaces exhibit

comparable slip resistance and may reasonably be classified as Class B surfaces in engineering design.

Overall, the test results provide quantitative experimental evidence for the influence of different faying-surface treatments on slip resistance and offer a clear numerical basis for selecting appropriate surface treatments in engineering practice and for refining slip-factor provisions in future revisions of design standards.

7. Limitations and Future Work

The present study still has several limitations. First, only six representative faying-surface treatment methods were examined, which may not fully capture the behaviour of emerging coating systems or the wider coating-thickness ranges used in engineering practice. Although all blasted surfaces were prepared to the same visual cleanliness level (Sa 2.5), quantitative roughness parameters (Ra and Rz) were not measured, limiting the ability to establish a direct correlation between surface texture and slip resistance.

All tests were performed under short-term static loading, without accounting for long-term environmental degradation, bolt-pretension relaxation, or cyclic loading effects, which may influence slip behaviour in service. In addition, the use of a single steel grade and simplified specimen geometry restricts the generalizability of the findings.

Furthermore, the experimental programme used a single representative dry-film thickness and a single curing duration for each coating system. The potential influences of multiple thickness levels—particularly for the epoxy zinc-rich (C type) and alcohol-soluble inorganic anti-slip (S type) coatings—and variations in curing duration on coating morphology, surface texture, and interfacial shear behaviour were not investigated. These parameters may significantly alter slip performance and, therefore, require systematic evaluation.

Future work will focus on: (1) expanding the investigation to a wider range of coating types, thickness levels, and curing regimes, with particular emphasis on epoxy zinc-rich and organic coating systems, in order to clarify the thickness-dependent degradation mechanisms of slip resistance; advanced thickness- and homogeneity-characterization methods, such as impedance spectroscopy [32], will be considered to improve the accuracy of coating quality assessment; (2) conducting long-term durability tests and cyclic slip loading to better reflect service conditions and to evaluate the evolution of slip resistance under repeated loading; (3) examining multiple steel grades and more realistic joint configurations to enhance the general applicability of the experimental findings; and (4) quantitatively measuring surface roughness parameters (Ra and Rz) and integrating these data with microscopic surface characterization techniques (e.g., SEM and 3D optical profilometry), enabling the establishment of a direct relationship between coating morphology, surface texture, and slip factor.

These efforts will help improve the applicability and reliability of slip-factor recommendations for engineering design.

Author Contributions: Conceptualization, L.L.; methodology, L.L.; formal analysis, Z.Y.; investigation, Z.Y., M.L., J.P. and S.D.; resources, L.L.; data curation, Z.Y.; writing—original draft preparation, L.L.; writing—review and editing, L.L.; funding acquisition, L.L. All authors have read and agreed to the published version of the manuscript.

Funding: This research received no external funding.

Data Availability Statement: The original contributions presented in the study are included in the article; further inquiries can be directed to the corresponding author.

Conflicts of Interest: The authors declare that they have no conflicts of interest.

References

1. Yu, S.; Lou, G.; Zhang, C. Experimental study on shear behavior of bolted friction-type high-strength connections after fire. *J. Disaster Prev. Mitig. Eng.* **2012**, *32*, 6–14. (In Chinese)
2. Lou, G.-B.; Zhu, M.-C.; Li, M.; Zhang, C.; Li, G.Q. Experimental research on slip-resistant bolted connections after fire. *J. Constr. Steel Res.* **2015**, *104*, 1–8. [CrossRef]
3. Lu, L.; Zhu, P.; Ding, S.; Ma, Z.; Li, R.; Nie, S.; Wang, W.; Raftery, G.M. Impact of anti-corrosion coatings and maintenance on high-strength bolt friction connections in C4 marine environment. *Structures* **2024**, *68*, 107098. [CrossRef]
4. Lu, L.; Nie, S.; Ding, S.; Ma, Z.; Li, R.; Wang, W.; Raftery, G. Corrosion degradation of shear performance in friction-type connections with high-strength bolts for steel structures. *J. Traffic Transp. Eng.* **2025**, *25*, 218–234. (In Chinese)
5. *T/CSCS 056-2024*; Technical Specification for Corrosion Protection of Steel Structures in Civil Buildings. China Association for Construction Standardization: Beijing, China, 2024. (In Chinese)
6. *JGJ 82-2011*; Technical Specification for High Strength Bolt Connections of Steel Structures. Ministry of Housing and Urban–Rural Development of the PRC: Beijing, China, 2011. (In Chinese)
7. *JTG D64-2015*; Specifications for Design of Highway Steel Bridge. Ministry of Transport of the PRC: Beijing, China, 2015. (In Chinese)
8. *GB 50017-2017*; Standard for Design of Steel Structures. China Architecture & Building Press: Beijing, China, 2017. (In Chinese)
9. *BS EN 1090-2:2018*; Execution of Steel Structures and Aluminium Structures—Part 2: Technical Requirements for Steel Structures. British Standards Institution: London, UK, 2018.
10. *ANSI/AISC 360-22*; Specification for Structural Steel Buildings. American Institute of Steel Construction: Chicago, IL, USA, 2022.
11. Annan, C.; Chiza, A. Slip resistance of metallized–galvanized faying surfaces in steel bridge construction. *J. Constr. Steel Res.* **2014**, *95*, 211–219. [CrossRef]
12. Wang, Y.; Wang, Y.; Chen, K.; Li, G.Q. Slip factors of high strength steels with shot blasted surface. *J. Constr. Steel Res.* **2019**, *157*, 10–18. [CrossRef]
13. Wang, Y.; Wang, Y.; Chen, K.; Li, G.Q. Slip factor between shot blasted mild steel and high strength steel surfaces. *J. Constr. Steel Res.* **2020**, *168*, 105969. [CrossRef]
14. Wang, Y.; Wang, Y.; Chen, K.; Jin, H.J. Slip factor of high strength steel with inorganic zinc-rich coating. *Thin-Walled Struct.* **2020**, *148*, 106595. [CrossRef]
15. Mahmoudi, M.; Kosari, M.; Lorestani, M.; Abad, M.J. Effect of contact surface type on the slip resistance in bolted connections. *J. Constr. Steel Res.* **2020**, *166*, 105943. [CrossRef]
16. Cao, X. Study on the Mechanical Behavior of High-Strength Steel Slip-Critical and Bolted Connections. Ph.D. Thesis, Chongqing University, Chongqing, China, 2022. (In Chinese).
17. Collini, L.; Garziera, R.; Corvi, A.; Cantarelli, G. Slip strength of COR-TEN and Zn-coated steel preloaded bolted joints. *Results Eng.* **2024**, *22*, 102009. [CrossRef]
18. Chen, X.; Shi, G.; Chen, Y. Experimental study on slip coefficient of high-strength steel bolt connection with arc thermal-sprayed aluminium contact surface. *Build. Struct.* **2021**, *51*, 87–92. (In Chinese)
19. Zheng, B.; Wang, J.; Gu, Y.; Shu, G.; Xie, J.; Jiang, Q. Experimental study on stainless steel high-strength bolted slip-resistant connections. *Eng. Struct.* **2021**, *231*, 111778. [CrossRef]
20. Zhang, Y.; Wang, Y.; Zhi, X.; Li, B.; Ouyang, Y. Tests on slip-resistant behaviour of aluminium alloy–stainless steel faying surfaces. *J. Constr. Steel Res.* **2023**, *202*, 107762. [CrossRef]
21. Han, Q.; Li, Y.; Lu, Y.; Wang, P. Effect of faying surface treatments and bolt tightened levels on fretting fatigue performance of slip critical connections with high strength bolts. *Tribol. Int.* **2025**, *201*, 110257. [CrossRef]
22. Takai, T. Dependence of slip behavior of bolted connection on contact pressure and splice plate thickness. *J. Constr. Steel Res.* **2026**, *237*, 110123. [CrossRef]
23. Georgiev, T. Practical issues in slip-resistant bolted connections for steel structures. *Build. Mater. Struct.* **2025**, *68*, 2400015G. [CrossRef]
24. Fuente, A.; Serrano-López, M.A.; López-Colina, C.; López-Gayarre, F. Slip-resistant connections: Comparison of friction areas in slip factor test specimens according to international codes. *ce/papers* **2024**, *7*, 124–133. [CrossRef]
25. Loo, W.; Quenneville, P.; Chouw, N. Influence of surface preparation and lubricating effect of mill scale on the performance of slip-friction connectors. *Constr. Build. Mater.* **2017**, *155*, 1025–1038. [CrossRef]
26. Wang, H.; Tang, F.; Qin, S.; Tu, K.; Guo, J. Corrosion-induced mechanical degradation of high-strength bolted steel connections. *J. Mater. Civ. Eng.* **2020**, *32*, 04020203. [CrossRef]
27. *ISO 8501-1*; Preparation of Steel Substrates Before Application of Paints and Related Products—Visual Assessment of Surface Cleanliness—Part 1: Rust Grades and Preparation Grades of Uncoated Steel Substrates and of Steel Substrates After Overall Removal of Previous Coatings. International Organization for Standardization: Geneva, Switzerland, 2007.

28. *ISO 8503-2*; Preparation of Steel Substrates Before Application of Paints and Related Products—Surface Roughness Characteristics of Blast-Cleaned Steel Substrates—Part 2: Method for the Grading of Surface Profile of Abrasive Blast-Cleaned Steel—Comparator Procedure. International Organization for Standardization: Geneva, Switzerland, 2012.
29. Xie, D.; Wang, J.; Hu, J.; Zhang, J. Influence of surface roughness on performance of zinc-rich paint coatings. *Trans. Nonferrous Met. Soc. China* **2002**, *12*, 1036–1039.
30. Montgomery, D.C. *Design and Analysis of Experiments*, 8th ed.; John Wiley & Sons: Hoboken, NJ, USA, 2013.
31. Annan, C.; Chiza, A. Characterization of slip resistance of high strength bolted connections with zinc-based metallized faying surfaces. *Eng. Struct.* **2013**, *56*, 2187–2196. [CrossRef]
32. Krbata, M.; Fabo, P.; Kohutiar, M.; Escherova, J.; Kuba, M.; Kianicova, M.; Eckert, M. Possibilities of Using Impedance Spectroscopy for Indirect Measurements of Thin Layers of Al & Cr-Al Coatings on Ni-based Superalloy Inconel 713LC Applied by the "Out-of-pack" Diffusion Method. *Manuf. Technol.* **2023**, *23*, 313–318.

Disclaimer/Publisher's Note: The statements, opinions and data contained in all publications are solely those of the individual author(s) and contributor(s) and not of MDPI and/or the editor(s). MDPI and/or the editor(s) disclaim responsibility for any injury to people or property resulting from any ideas, methods, instructions or products referred to in the content.